# Polymer Chemistry



PAPER View Article Online
View Journal | View Issue



**Cite this:** *Polym. Chem.*, 2025, **16**, 174

Received 11th October 2024, Accepted 22nd November 2024 DOI: 10.1039/d4py01140f rsc.li/polymers

# Controlling thiyl radical polymerization via in situ desulfurization †

Huajuan Hu, a,b Ping Yi, a,b Jiayang He, Derong Cao \*a and Hanchu Huang \*b \*b

Controlling thiyl radical polymerizations is highly desirable for synthesizing polymers with precisely controlled main-chain structures, yet it remains challenging due to the difficulty of reversibly controlling propagating thiyl radicals with existing methods. Here, we present a new strategy in which the propagating thiyl radical undergoes desulfurization with trivalent phosphorus, generating a stabilized carbon radical for reversible control. This approach enables the radical ring-opening polymerization of macrocyclic allylic sulfides to be effectively regulated by reversible addition—fragmentation chain transfer (RAFT) agents, resulting in polymers with well-defined architectures, which was exemplified by the successful incorporation of sequence-defined segments into the polymer backbone, along with diblock copolymerization of macrocyclic allylic sulfides. This work will further advance thiyl radical polymerizations toward polymers with controlled main-chain functionalities.

#### Introduction

Thivl radical polymerizations represent a class of chain-growth polymerization reactions that propagate via thiyl radicals and have attracted growing attention in recent years because of their potential applications in synthesizing polymers with extended main-chain structural motifs compared with carbon radical polymerizations. 1-14 Despite this promising prospect, thivl radical polymerizations are challenging to regulate by traditional reversible-deactivation radical polymerization (RDRP) techniques. 15-21 Consequently, these polymerizations often encounter poor control over the molecular weight and dispersity of the resulting polymers, thereby limiting their ability to produce materials with precisely defined structures. To address this challenge, we recently proposed a strategy that in situ converts the propagating thiyl radical into a stabilized carbon radical capable of reversible control, thereby enabling thiyl radical polymerizations to be regulated by reversible addition-fragmentation chain transfer (RAFT) agents (Fig. 1A).<sup>22</sup> Although this strategy is highly efficient, desulfurization agents are still limited to isocyanides, which are both costly and emit an unpleasant odor, thus diminishing the

Trivalent phosphorus compounds are among the most important classes of reagents in organic synthesis. <sup>23–28</sup> They are readily accessible and well-known as significant ligands in transition metal-catalyzed reactions, while their extensive use as mediators in radical reactions is less known. <sup>29–31</sup> These advancements can be traced back to the 1950s, when Walling <sup>32–34</sup> and Hoffman <sup>35</sup> made a significant discovery by demonstrating that alkyl thiyl radicals could be efficiently trapped by trivalent phosphorus, resulting in the cleavage of the C–S bond and the generation of carbon radicals. Subsequently, various bond transformations through radical desulfurization have been successively reported over the past decades, further demonstrating the high efficiency of this strategy. <sup>36–44</sup> However, to our knowledge, the applications of this strategy in regulating thiyl radical polymerizations remain

(B) This work: in situ desulfurization by adding trivalent phosphorus

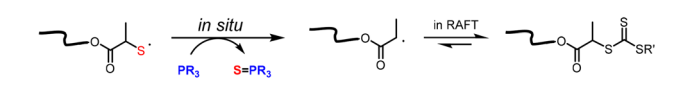


Fig. 1 Approaches for controlling thiyl radical polymerizations.

practicality of this approach. Therefore, expanding the scope of desulfurization agents is necessary to apply this approach more universally.

<sup>&</sup>lt;sup>a</sup>State Key Laboratory of Luminescent Materials and Devices, School of Chemistry and Chemical Engineering, South China University of Technology, Guangzhou 510640, China. E-mail: drcao@scut.edu.cn

bSchool of Materials Science and Engineering, Key Laboratory for Polymeric Composite and Functional Materials of Ministry of Education, Sun Yat-sen University, Guangzhou 510006, China. E-mail: huanghch9@mail.sysu.edu.cn † Electronic supplementary information (ESI) available. See DOI: https://doi.org/10.1039/d4py01140f

<sup>(</sup>A) Previous work: in situ desulfurization by adding isocyanides

**Polymer Chemistry** Paper

largely unexplored. On the basis of our new findings and previous studies on phosphorus-mediated radical desulfurization, we envisaged that trivalent phosphorus could also serve as an effective desulfurization agent for the in situ generation of carbon radicals during thiyl radical polymerizations (Fig. 1B).

Herein, we realize this goal and employ trivalent phosphorus as a desulfurization agent to convert thiyl radicals into carbon radicals during the polymerization process, thereby enabling the radical ring-opening polymerization of macrocyclic allylic sulfides to be controlled by RAFT agents. Systematic optimization of reaction conditions allowed effective control over the molecular weight and dispersity of the resulting polymers. The versatility of this approach was further demonstrated through the successful incorporation of various functional groups into the polymer backbone, along with the radical diblock copolymerization of macrocyclic monomers. Density functional theory (DFT) calculations indicated that the capture of thiyl radicals by trivalent phosphorus occurs through a kinetically and thermodynamically favorable concerted mechanism.

# **Experimental**

#### **Materials**

Unless otherwise noted, organic solvents such as dimethyl sulfoxide (DMSO), N,N-dimethylformamide (DMF), tetrahydrofuran (THF), toluene, and dioxane were of analytical purity grade and used as received. Azobis(isobutyronitrile) (AIBN) was recrystallized from methanol before use. Other commercially available reagents were used without further purification. Thin layer chromatography (TLC) was performed using Huanghai TLC silica gel plates (SHGF254) and visualized using UV light.

#### Characterization

<sup>1</sup>H and <sup>13</sup>C NMR spectra were recorded using a Bruker AV400 FT-NMR spectrometer with CDCl<sub>3</sub> as the solvent at room temperature, and the chemical shifts were given in ppm. The residual solvent signals were used as references (CDCl<sub>3</sub>:  $\delta_{\rm H}$  = 7.26 ppm and  $\delta_{\rm C}$  = 77.16 ppm). Size exclusion chromatography (SEC) measurements were performed using a Shimadzu highperformance SEC system HLC-8320SEC with an LC-20AD pump at 40 °C and a flow rate of 0.6 mL min<sup>-1</sup>. HPLC grade tetrahydrofuran (THF) was used as the eluent. Polystyrene standards (Shodex, SM-105) were used to determine the molecular weight and molecular weight distribution of polymers. The polymers were dissolved in the THF solution and filtered through a 0.45 µm PTFE filter before being injected into the SEC system. Matrix-assisted laser desorption/ionization timeof-flight (MALDI-TOF) mass spectrometry was performed using a Bruker UltrafleXtreme mass spectrometer.

#### **Computational methods**

Unless otherwise noted, all quantum chemical calculations were carried out with the Gaussian 16 computer program.<sup>45</sup> The geometry optimization and frequency calculations were

performed at the M06-2X/def2-SVP level with the solvation model based on density (SMD) in DMSO. 46,47 All computed frequencies are real except the transition state structures, which have one imaginary frequency. The connectivity between each transition state and its two neighboring stationary points was confirmed by intrinsic reaction coordinate (IRC) calculations. Single-point energies were calculated at the PWPB95-D3(BJ)/ def2-TZVPP level with the SMD in DMSO, 48-50 and the calculations were carried out using the ORCA 5.0.4 computer program. 51,52 Thermal corrections were implemented with Shermo software<sup>53</sup> using a scale factor of 0.9762 <sup>54</sup> and Grimme's quasi-harmonic oscillator approximation<sup>55</sup> at a temperature of 343.15 K and a concentration of 1 mol  $L^{-1}$ .

#### General procedure for controlled radical polymerization

All polymerization reactions were performed under a nitrogen atmosphere using a standard Schlenk technique. A stock solution of 4-cyano-4-(((dodecylthio)carbonothioyl)thio)pentanoic acid (CTA1) and a stock solution of AIBN were prepared in degassed DMSO at 0.04 M and 0.04 M, respectively. A typical procedure for the preparation of P1 is given below as an example. A 10 mL Schlenk vial equipped with a stir bar was charged with macrocyclic monomer 1 (0.1 mmol), followed by the stock solution of CTA1 (0.04 M, 125 µL), AIBN (0.04 M, 125  $\mu$ L), triethyl phosphite (0.12 mmol) and DMSO (750  $\mu$ L). The vial was then sealed. The solution was deoxygenated via three freeze-pump-thaw cycles, backfilled with nitrogen, and then heated at 70 °C for a given time. After the reaction, the vial was cooled in an ice bath and opened to air to stop the polymerization. The reaction mixture was diluted with a minimum amount of DCM and precipitated in diethyl ether. The obtained solid was re-dissolved in a minimum amount of DCM for further precipitation, yielding the polymer that was then characterized using SEC and NMR.

#### Results and discussion

We commenced our investigation by exploring the feasibility of the polymerization with the use of monomer 1 as the model substrate. Notably, multigram quantities of monomer 1 were readily obtained using saccharin as the starting material (Schemes S1 and S2†). Building on the conditions established in our previous work,22 we then examined the radical ringopening polymerization of monomer 1 under various reaction conditions, with representative results summarized in Table 1 (see the ESI† for more details). The polymerization was initially carried out at 70 °C in the presence of AIBN and triethyl phosphite in DMSO under a nitrogen atmosphere, successfully yielding polymer P1 with a number-average molecular weight  $(M_n)$  of 10.2 kDa and a dispersity (D) of 2.05 (Table 1, entry 1). Introducing the RAFT agent CTA1 into the reaction reduced the dispersity to 1.42, indicating that the polymerization has been controlled by CTA1 (Table 1, entry 2). Note that whether the polymerization was truly controlled still requires further investigation through kinetic studies,56 which will be

Table 1 Experimental conditions and results of the polymerization

| Entry <sup>a</sup> | Monomer | [M]/[CTA]/[AIBN] | $PR_3$     | RAFT agent | Solvent | Time | Conversion <sup>b</sup> | $M_{ m n,Theo}^{\ \ c}$ | $M_{ m n,SEC}^{d}$ | $\mathcal{D}^d$ |
|--------------------|---------|------------------|------------|------------|---------|------|-------------------------|-------------------------|--------------------|-----------------|
| 1                  | 1       | 20/0/1           | $P(OEt)_3$ | _          | DMSO    | 48 h | 80%                     | _                       | 10 200             | 2.05            |
| 2                  | 1       | 20/1/1           | $P(OEt)_3$ | CTA1       | DMSO    | 25 h | 80%                     | 8400                    | 7900               | 1.42            |
| 3                  | 1       | 20/1/1           | $P(OEt)_3$ | CTA2       | DMSO    | 25 h | 80%                     | 8300                    | 6700               | 1.38            |
| 4                  | 1       | 20/1/1           | $P(OEt)_3$ | CTA3       | DMSO    | 25 h | 81%                     | 8300                    | 6600               | 1.42            |
| 5                  | 1       | 20/1/1           | $P(OEt)_3$ | CTA4       | DMSO    | 25 h | 81%                     | 8400                    | 6700               | 1.39            |
| 6                  | 1       | 20/1/1           | $PPh_3$    | CTA1       | DMSO    | 25 h | 82%                     | 8600                    | 6300               | 1.43            |
| 7                  | 1       | 20/1/1           | $PPh_2Pr$  | CTA1       | DMSO    | 25 h | 78%                     | 8200                    | 6800               | 1.44            |
| 8                  | 1       | 20/1/1           | $PPhMe_2$  | CTA1       | DMSO    | 25 h | 67%                     | 7100                    | 6500               | 1.36            |
| 9                  | 1       | 20/1/1           | $P(OEt)_3$ | CTA1       | DMSO    | 12 h | 79%                     | 8300                    | 7800               | 1.41            |
| 10                 | 1       | 20/1/1           | $P(OEt)_3$ | CTA1       | DMF     | 12 h | 62%                     | 6600                    | 6000               | 1.40            |
| 11                 | 1       | 20/1/1           | $P(OEt)_3$ | CTA1       | Dioxane | 12 h | 68%                     | 7200                    | 7900               | 1.40            |
| 12                 | 1       | 20/1/1           | $P(OEt)_3$ | CTA1       | THF     | 12 h | 57%                     | 6100                    | 5900               | 1.33            |
| 13                 | 1       | 20/1/1           | $P(OEt)_3$ | CTA1       | Toluene | 12 h | <5%                     |                         | _                  | _               |
| 14                 | 1       | 10/1/0.3         | $P(OEt)_3$ | CTA1       | DMSO    | 12 h | 69%                     | 3800                    | 6100               | 1.22            |
| 15                 | 1       | 20/1/0.3         | $P(OEt)_3$ | CTA1       | DMSO    | 12 h | 50%                     | 5400                    | 8100               | 1.27            |
| 16                 | 1       | 50/1/0.3         | $P(OEt)_3$ | CTA1       | DMSO    | 24 h | 46%                     | 11 900                  | 9900               | 1.40            |
| 17                 | 1       | 100/1/0.5        | $P(OEt)_3$ | CTA1       | DMSO    | 24 h | 41%                     | 21 500                  | 13 500             | 1.54            |
| 18                 | 2       | 10/1/0.3         | $P(OEt)_3$ | CTA1       | DMSO    | 12 h | 65%                     | 4000                    | 8000               | 1.26            |
| 19                 | 2       | 20/1/0.3         | $P(OEt)_3$ | CTA1       | DMSO    | 12 h | 55%                     | 6500                    | 10400              | 1.33            |
| 20                 | 2       | 50/1/0.3         | $P(OEt)_3$ | CTA1       | DMSO    | 12 h | 32%                     | 9300                    | 13 600             | 1.38            |
| 21                 | 2       | 100/1/0.3        | $P(OEt)_3$ | CTA1       | DMSO    | 12 h | 23%                     | 13 200                  | 14 700             | 1.48            |
| 22                 | 3       | 10/1/0.3         | $P(OEt)_3$ | CTA1       | DMSO    | 12 h | 77%                     | 5600                    | 11 200             | 1.30            |
| 23                 | 3       | 20/1/0.3         | $P(OEt)_3$ | CTA1       | DMSO    | 12 h | 61%                     | 8600                    | 14 300             | 1.39            |
| 24                 | 3       | 50/1/0.3         | $P(OEt)_3$ | CTA1       | DMSO    | 12 h | 49%                     | 16 800                  | 17 900             | 1.42            |
| 25                 | 3       | 100/1/0.5        | $P(OEt)_3$ | CTA1       | DMSO    | 12 h | 42%                     | 28 600                  | 18 300             | 1.49            |

<sup>a</sup> Experimental conditions: [M] = 0.1 M at 70 °C under a nitrogen atmosphere unless otherwise noted. <sup>b</sup> Monomer conversion was determined by <sup>1</sup>H NMR spectroscopy. <sup>c</sup> Calculated following the equation:  $M_{n,\text{theo}} = [M]_0/[\text{CTA}]_0 \times \text{MW}^M' \times \text{conversion} + \text{MW}^{\text{CTA}}$ , where [M]<sub>0</sub>, [CTA]<sub>0</sub>, MW<sup>M'</sup>, and MW<sup>CTA</sup> correspond to the initial monomer concentration, CTA concentration, average molar mass of the monomer and desulfurization unit, and molar mass of CTA, respectively. <sup>d</sup> Molecular weight and dispersity were determined by size-exclusion chromatography (SEC) analysis calibrated to polystyrene standards.

addressed in Fig. 2. The polymerization could also be effectively regulated using other RAFT agents, such as CTA2-CTA4, demonstrating the broad applicability of RAFT agents in controlling this polymerization (Table 1, entries 3-5). Among the trivalent phosphorus compounds tested, triethyl phosphite was identified as the optimal choice due to its polymerization efficiency and commercial availability (Table 1, entries 6-8). Further screening of solvents revealed that the polymerization also proceeded well in DMF, THF, and dioxane, while no polymerization occurred in toluene due to the low solubility of monomers and polymers in this solvent (Table 1, entries 9-13). Consistent with controlled polymerization, we were able to regulate the molecular weight of P1 by adjusting the

monomer/CTA ratios (Table 1, entries 14–17). Notably, compared to the isocyanides employed in our previous research, <sup>22</sup> trivalent phosphorus is not only commercially accessible but also exhibits high efficiency for radical desulfurization, facilitating the production of polymers with relatively high molecular weights.

With suitable polymerization conditions identified, we next explored the scope and versatility of the polymerization. One of the key advantages of this method is its ability to polymerize macrocyclic monomers with less ring strain, as the efficiency of polymerization relies on the effectiveness of the ringopening trigger. We hypothesized that even larger ring-sized monomers could be efficiently polymerized under these

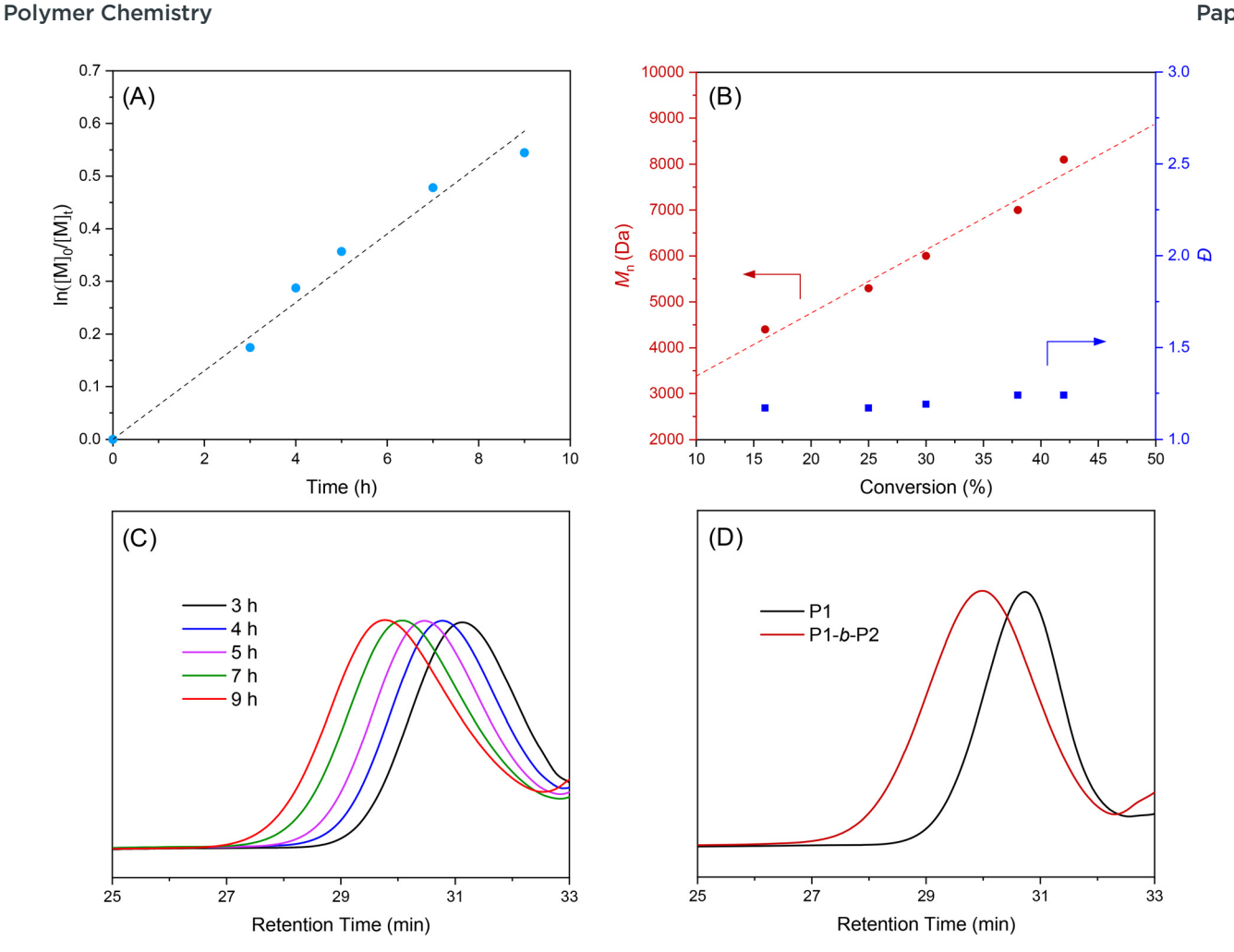


Fig. 2 (A) The plot of  $\ln([M]_0/[M]_t)$  versus reaction time for the polymerization of monomer 1. (B) Plots of  $M_n$  (red) and D (blue) versus monomer conversion for the polymerization of monomer 1. (C) SEC traces for the kinetic study. (D) SEC traces for the diblock copolymerization.

conditions. Indeed, we found that macrocyclic monomer 2, with a 20-membered ring, successfully polymerized to produce polymer **P2** ( $M_n = 8.0$  kDa and D = 1.26), and a higher molecular weight ( $M_n$  = 14.7 kDa and D = 1.48) was achieved at a monomer/CTA ratio of 100/1 (Table 1, entries 18-21). Another unique aspect of this polymerization is its ability to control the functionality within the polymer backbone. To test this, we designed and synthesized macrocyclic monomer 3, which includes the ring-opening trigger along with 3-aminopropanol, succinic acid, and butane-1,4-diol units, resulting in an ABCD sequence within the polymer backbone after polymerization. As expected, this monomer polymerized efficiently under the established conditions, yielding sequence-defined polymers P3 with good control over molecular weights (Table 1, entries 22-25). These polymers, which are difficult to obtain using traditional radical ring-opening polymerizations, demonstrate the potential of our polymerization strategy for accessing complex, sequence-specific functional polymers.

To further confirm the controlled nature of the polymerization, we studied the kinetics by sampling the reaction at various time intervals. The polymerization exhibited first-order kinetic behavior with a linear increase in  $M_n$  as conversion progressed while maintaining relatively low dispersity, indicating effective control over the polymerization process. Additionally, matrix-assisted laser desorption/ionization timeof-flight (MALDI-TOF) mass spectrometry was used to analyze the microstructure of P1, revealing high chain-end fidelity in the individual polymers (Fig. S15†). This underscores the high efficiency of RAFT agents in regulating the chain-growth process. An essential characteristic of controlled polymerization is the ability to extend from intact chain-end groups. To demonstrate this, we first synthesized a macromolecular CTA, **P1** ( $M_{\rm n}$  = 5.8 kDa and D = 1.11), through the homopolymerization of monomer 1. This polymer was subsequently extended using monomer 2, successfully producing a diblock copolymer P1-b-P2 ( $M_n = 8.0$  kDa and D = 1.22, Fig. 2D). This outcome highlights the potential of this approach for synthesizing polymers with well-defined architectures.

Next, DFT calculations were conducted to investigate the chain propagation process and further provide insight into the origin of radical desulfurization (Fig. 3). 57-59 The calculations indicated that the capture of the thiyl radical by triethyl phos-

Fig. 3 Calculated free energy profiles for the chain-growth process and the values given in kcal mol<sup>-1</sup> are the relative free energies.

phite occurs via a concerted mechanism, which exhibits a lower energy barrier (TS1, 6.8 kcal mol<sup>-1</sup>) compared to that for the direct addition of the thiyl radical to the monomer (TS5, 9.9 kcal mol<sup>-1</sup>). This finding suggests that radical desulfurization is kinetically more favorable. In addition, this desulfurization process is thermodynamically favorable due to a strong P=S bond formed after desulfurization. Consequently, the thiyl radical preferentially reacts with triethyl phosphite, desulfurizing and yielding carbon radical intermediate Int1. Notably, the desulfurization using isocyanides in our previous work was found to be kinetically unfavorable.<sup>22</sup> In contrast, the desulfurization using trivalent phosphorus in this work was kinetically favorable, further supporting the high efficiency of trivalent phosphorus in desulfurization. Subsequently, Int1 attacks monomer 1 through TS2 with an energy barrier of 16.6 kcal mol<sup>-1</sup> to form Int2. An alternative pathway that is more energetically favorable involves the reversible deactivation of Int1 by the RAFT agent (Int1-TS8-Int8), characterized by an energy barrier of 12.3 kcal mol<sup>-1</sup>, thereby allowing for good control over the polymerization processes. Subsequently, Int2 undergoes rapid and energetically favorable radical cyclization, leading to the formation of Int3. Finally, β-elimination of Int3 occurs via TS4 with an energy barrier of 9.9 kcal mol<sup>-1</sup>, resulting in the ring-opening of the macrocycle

and the generation of a propagating thiyl radical for the next propagation cycle. Overall, the calculated results align well with experimental findings, providing valuable mechanistic insights into the chain-growth process.

#### Conclusions

In summary, we have developed a new strategy that effectively enables the control of thiyl radical polymerizations using existing RDRP techniques. This approach relies on the desulfurization of the propagating thiyl radical with trivalent phosphorus, generating a carbon radical capable of reversible control, which facilitates precise regulation of the radical ring-opening polymerization of macrocyclic allylic sulfides through the RAFT process. The versatility of this protocol was further demonstrated by the successful synthesis of diblock copolymers and the incorporation of sequence-defined segments into the polymer backbone. Additionally, DFT calculations confirmed that the desulfurization process occurs through a kinetically and thermodynamically favorable concerted mechanism. Considering the availability of trivalent phosphorus, we anticipate that this method will provide a facile route to the

controlled synthesis of complex main-chain functional polymers.

#### **Author contributions**

H. Hu, P. Yi, and J. He performed the experiments and collected the data. H. Huang and D. Cao supervised the project and wrote the manuscript. All authors have given approval to the final version of the manuscript.

## Data availability

The data supporting this article have been included as part of the ESI.†

### Conflicts of interest

There are no conflicts to declare.

# Acknowledgements

This research was funded by the National Natural Science Foundation of China (22471299 and 22071066) and the Guangdong Basic and Applied Basic Research Foundation (2023A1515012157).

#### References

- 1 A. Tardy, J. Nicolas, D. Gigmes, C. Lefay and Y. Guillaneuf, Chem. Rev., 2017, 117, 1319-1406.
- 2 T. Pesenti and J. Nicolas, ACS Macro Lett., 2020, 9, 1812-1835.
- 3 T.-J. Yue, W.-M. Ren and X.-B. Lu, Chem. Rev., 2023, 123, 14038-14083.
- 4 P. T. Do, B. L. J. Poad and H. Frisch, Angew. Chem., Int. Ed., 2023, **62**, e202213511.
- 5 F. Sbordone, J. Veskova, B. Richardson, P. T. Do, A. Micallef and H. Frisch, J. Am. Chem. Soc., 2023, 145, 6221-6229.
- 6 F. Sbordone, A. Micallef and H. Frisch, Angew. Chem., Int. Ed., 2024, 63, e202319839.
- 7 P. T. Do, F. Sbordone, H. Kalmer, A. Sokolova, C. Zhang, L. D. Thai, D. V. Golberg, R. Chapman, B. L. J. Poad and H. Frisch, Chem. Sci., 2024, 15, 12410-12419.
- 8 K.-X. Chen, C.-H. Cui, Z. Li, T. Xu, H.-Q. Teng, Z.-Y. He, Y.-Z. Guo, X.-Q. Ming, Z.-S. Ge, Y.-F. Zhang and T.-J. Wang, Chin. J. Polym. Sci., 2024, 42, 1479-1487.
- 9 R. Zhang, S. Liu, C. Zhuo, H. Cao and X. Wang, Macromolecules, 2024, 57, 132-141.
- 10 S. Zhang, C. Cao, S. Jiang and H. Huang, Macromolecules, 2022, 55, 9411-9419.
- 11 Z. Cai, S. Jiang, J. Zhang, J. He, Y. Bai and H. Huang, Polym. Chem., 2023, 14, 3117-3125.

- 12 S. Jiang and H. Huang, Angew. Chem., Int. Ed., 2023, 62, e202217895.
- 13 H. Mutlu, E. B. Ceper, X. Li, J. Yang, W. Dong, M. M. Ozmen and P. Theato, Macromol. Rapid Commun., 2019, 40, 1800650.
- 14 X. Fu, A. Qin and B. Z. Tang, Aggregate, 2023, 4, e350.
- 15 C. Lefay and Y. Guillaneuf, Prog. Polym. Sci., 2023, 147,
- 16 F. Sbordone and H. Frisch, Chem. Eur. J., 2024, 30, e202401547.
- 17 H. Huang, Acta Polym. Sin., 2024, 55, DOI: 10.11777/j. issn1000-3304.2024.24211.
- 18 H. Huang, B. Sun, Y. Huang and J. Niu, J. Am. Chem. Soc., 2018, 140, 10402-10406.
- 19 H. Huang, W. Wang, Z. Zhou, B. Sun, M. An, F. Haeffner and J. Niu, J. Am. Chem. Soc., 2019, 141, 12493-12497
- 20 Y. Wang, J. Du and H. Huang, Angew. Chem., Int. Ed., 2024, 63, e202318898.
- 21 S. Jiang and H. Huang, Polymer, 2024, 303, 127106.
- 22 S. Zhang, Y. Wang, H. Huang and D. Cao, Angew. Chem., Int. Ed., 2023, 62, e202308524.
- 23 B. E. Ivanov and V. F. Zheltukhin, Russ. Chem. Rev., 1970,
- 24 V. F. Mironov, I. V. Konovalova, L. M. Burnaeva and E. N. Ofitserov, Russ. Chem. Rev., 1996, 65, 935.
- 25 D. Basavaiah and G. Veeraraghavaiah, Chem. Soc. Rev., 2011, 41, 68-78.
- 26 G. Zeng, S. Maeda, T. Taketsugu and S. Sakaki, Angew. Chem., Int. Ed., 2014, 53, 4633-4637.
- 27 H. Ni, W.-L. Chan and Y. Lu, Chem. Rev., 2018, 118, 9344-
- 28 H. Guo, Y. C. Fan, Z. Sun, Y. Wu and O. Kwon, Chem. Rev., 2018, 118, 10049-10293.
- 29 D. Leca, L. Fensterbank, E. Lacôte and M. Malacria, Chem. Soc. Rev., 2005, 34, 858.
- 30 K. Luo, W.-C. Yang and L. Wu, Asian J. Org. Chem., 2017, 6, 350-367.
- 31 J. A. Rossi-Ashton, A. K. Clarke, W. P. Unsworth and R. J. K. Taylor, ACS Catal., 2020, 10, 7250-7261.
- 32 C. Walling and R. Rabinowitz, J. Am. Chem. Soc., 1957, 79, 5326-5326.
- 33 C. Walling and R. Rabinowitz, J. Am. Chem. Soc., 1959, 81, 1243-1249.
- 34 C. Walling, O. H. Basedow and E. S. Savas, J. Am. Chem. Soc., 1960, 82, 2181-2184.
- 35 F. W. Hoffmann, R. J. Ess, T. C. Simmons and R. S. Hanzel, J. Am. Chem. Soc., 1956, 78, 6414-6414.
- 36 A. González and G. Valencia, Tetrahedron: Asymmetry, 1998, 9, 2761-2764.
- 37 J. Cuesta, G. Arsequell, G. Valencia and A. González, Tetrahedron: Asymmetry, 1999, 10, 2643-2646.
- 38 G. Arsequell, A. González and G. Valencia, Tetrahedron Lett., 2001, 42, 2685-2687.
- 39 Q. Wan and S. J. Danishefsky, Angew. Chem., Int. Ed., 2007, 46, 9248-9252.

- 40 X.-F. Gao, J.-J. Du, Z. Liu and J. Guo, *Org. Lett.*, 2016, **18**, 1166–1169
- 41 L. Zhang, X. Si, Y. Yang, S. Witzel, K. Sekine, M. Rudolph, F. Rominger and A. S. K. Hashmi, *ACS Catal.*, 2019, 9, 6118–6123.
- 42 Q. Qin, W. Wang, C. Zhang, S. Song and N. Jiao, *Chem. Commun.*, 2019, 55, 10583–10586.
- 43 W. Qiu, S. Shi, R. Li, X. Lin, L. Rao and Z. Sun, *Chin. J. Chem.*, 2021, 39, 1255–1258.
- 44 Z. Sun, W. Ma, Y. Cao, T. Wei, X. Mo, H. Y. Chow, Y. Tan, C. H. P. Cheung, J. Liu, H. K. Lee, E. C. M. Tse, H. Liu and X. Li, *Chem*, 2022, 8, 2542–2557.
- 45 M. J. Frisch, G. W. Trucks, H. B. Schlegel, G. E. Scuseria, M. A. Robb, J. R. Cheeseman, G. Scalmani, V. Barone, B. Mennucci, G. A. Petersson, H. Nakatsuji, M. Caricato, X. Li, H. P. Hratchian, A. F. Izmaylov, J. Bloino, G. Zheng, J. L. Sonnenberg, M. Hada, M. Ehara, K. Toyota, R. Fukuda, J. Hasegawa, M. Ishida, T. Nakajima, Y. Honda, O. Kitao, H. Nakai, T. Vreven, J. A. Montgomery Jr., J. E. Peralta, F. Ogliaro, M. Bearpark, J. J. Heyd, E. Brothers, K. N. Kudin, V. N. Staroverov, R. Kobayashi, J. Normand, K. Raghavachari, A. Rendell, J. C. Burant, S. S. Iyengar, J. Tomasi, M. Cossi, N. Rega, J. M. Millam, M. Klene, J. E. Knox, J. B. Cross, V. Bakken, C. Adamo, J. Jaramillo, R. Gomperts, R. E. Stratmann, O. Yazyev, A. J. Austin, R. Cammi, C. Pomelli, J. W. Ochterski, R. L. Martin, K. Morokuma, V. G. Zakrzewski, G. A. Voth, P. Salvador, J. J. Dannenberg, S. Dapprich, A. D. Daniels, O. Farkas, J. B. Foresman, J. V. Ortiz, J. Cioslowski and D. J. Fox, Gaussian 16, Gaussian, Inc., Wallingford, CT, 2016.

- 46 F. Weigend and R. Ahlrichs, *Phys. Chem. Chem. Phys.*, 2005, 7, 3297–3305.
- 47 Y. Zhao and D. G. Truhlar, *Theor. Chem. Acc.*, 2008, **120**, 215-241.
- 48 S. Grimme, J. Antony, S. Ehrlich and H. Krieg, *J. Chem. Phys.*, 2010, **132**, 154104.
- 49 L. Goerigk and S. Grimme, J. Chem. Theory Comput., 2011, 7, 291–309.
- 50 S. Grimme, S. Ehrlich and L. Goerigk, *J. Comput. Chem.*, 2011, 32, 1456–1465.
- 51 F. Neese, Wiley Interdiscip. Rev.: Comput. Mol. Sci., 2012, 2, 73–78.
- 52 F. Neese, Wiley Interdiscip. Rev.: Comput. Mol. Sci., 2022, 12, e1606.
- 53 T. Lu and Q. Chen, Comput. Theor. Chem., 2021, 1200, 113249.
- 54 M. K. Kesharwani, B. Brauer and J. M. L. Martin, *J. Phys. Chem. A*, 2015, **119**, 1701–1714.
- 55 S. Grimme, Chem. Eur. J., 2012, 18, 9955-9964.
- 56 M. Fellows, R. G. Jones, D. J. Keddie, C. K. Luscombe, J. B. Matson, K. Matyjaszewski, J. Merna, G. Moad, T. Nakano, S. Penczek, G. T. Russell and P. D. Topham, *Pure Appl. Chem.*, 2022, 94, 1093– 1147.
- 57 S. Han, M. Xu and M. Chen, *Acta Polym. Sin.*, 2024, 55, 841–855.
- 58 M. Bursch, J.-M. Mewes, A. Hansen and S. Grimme, *Angew. Chem.*, *Int. Ed.*, 2022, **61**, e202205735.
- 59 Y. Zhao and D. G. Truhlar, Acc. Chem. Res., 2008, 41, 157-167.